2017 IEEE/RSJ International Conference on Intelligent Robots and Systems (IROS)
September 24–28, 2017, Vancouver, BC, Canada

Bipedal Walking Control against Swing Foot Collision Using Swing Foot Trajectory Regeneration and Impact Mitigation

Tatsuya Ishikawa, Yuta Kojio, Kunio Kojima,
Shunichi Nozawa, Yohei Kakiuchi, Kei Okada and Masayuki Inaba

***Abstract*— For humanoid robots, unexpected collision can cause instability of robot balancing and damage to both robots and environment. This paper presents a reactive bipedal walking controller against swing foot collision for humanoid robots. This controller is composed of following three components: 1) Swing Foot Trajectory Regenerator, 2) Swing Foot Collision Detector, and 3) Swing Foot Impact Mitigation Controller. By regenerating swing foot trajectory depending on situations, humanoid robots can avoid falling down. However, although humanoid robots detect collision and regenerate a swing foot, collision impact can cause bad effects such as damage and posture rotation. Therefore, to mitigate strong impact, we propose Swing Foot Impact Mitigation Controller, which is composed of two controllers. The proposed method is validated through the experiments by actual humanoid robot CHIDORI. We confirm that CHIDORI can avoid falling down against collision in two situations: walking on the flat ground, and stepping up a stair.**

I. INTRODUCTION

For humanoid robots to work in human environments with us, the walking stabilization control against disturbances is essential. When humanoid robots walk, we compute the footstep plan with environmental recognition to avoid obstacles. However, owing to odometry errors which can be caused by poor accuracy of recognition and software or hardware faults, unexpected collisions may occur. In particular, a swing leg is the region which is most likely to collide with obstacles such as Fig.1.

Several studies have achieved stable walking in uneven terrain against vertical collisions of the swing foot. Kajita *et al.*[1] proposed stabilization control by modifying a desired zero moment point (ZMP) on the basis of the Linear Inverted Pendulum Model (LIP) [2] and realized the ZMP by foot force and torque control. Nishiwaki *et al.*[3] realized walking on uneven terrains by short cycle walking pattern regeneration which uses posture control and center of pressure control for stable contacts.

Against large disturbances humanoid robots must take steps or modify landing points appropriately. Pratt *et al.*[4] proposed Capture Point, which is the point where humanoid robots come to a complete stop. Some researchers, furthermore, discuss a standing stability taking supporting regions into account[5][6].

Although these researches have dealt with stabilization against vertical collisions, horizontal collisions like a stumble are not taken into account. In contrast, Morisawa *et al.*[7] focused on horizontal collisions of a swing foot using the reactive pattern generation of the center of gravity (COG), ZMP and a swing motion. However, they did not consider the safety of a landing point and obstacles higher than the planned swing foot height. To deal with this problem, regenerating swing foot trajectory is essential.

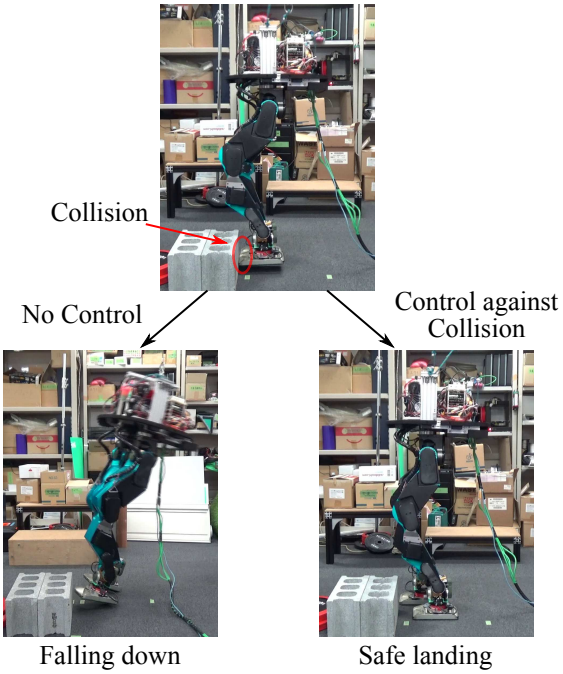

Fig. 1: Swing foot collision during walking

In addition, they did not consider bad effects of strong impact during fast walking either. When a swing foot has a strong impact, humanoid robots may rotate around vertical (yaw) axis. A lot of dynamic models such as LIP do not consider the rotation around yaw axis, therefore impact mitigation against swing foot collisions is also essential. To mitigate the impact on a swing foot, some approaches to realize backdrivability of joints have been proposed. Although they are effective, they require the particular actuators such as the SEA[8] or the torque sensors[9] and therefore we cannot use them for a lot of position-controlled humanoid robots.

Based on the above, we propose the controller to regenerate swing foot trajectory, to detect swing foot collision and to mitigate impact on a swing foot against swing foot collision. This paper is organized as follows: Section II introduces our experimental humanoid robot CHIDORI and

T. Ishikawa, Y. Kojio, K. Kojima, S. Nozawa, Y. Kakiuchi, K. Okada and M. Inaba are with Department of Mechano-Infomatics, The University of Tokyo, 7-3-1 Hongo, Bunkyo-ku, Tokyo 113-8656, Japan ishikawa at jsk.imi.i.u-tokyo.ac.jp

the proposed system of this study. Section III explains how to generate/regenerate the swing foot trajectory, the landing point modification based on Capture Point, and the swing foot collision detection. Section IV introduces the swing foot impact mitigation controller. Section V shows experimental results with the proposed methods. Section VI concludes this paper.

II. Experimental Robot and System Architecture

A. Life-Size Biped Robot CHIDORI

The experimental robot for this study is CHIDORI shown in Fig.1, which is designed based on STARO[10]. CHIDORI is about 1.3m tall, weighs approximately 50kg, and has 12 degrees of freedom. The motor-driven system of each joint is derived from the water-cooled high power system[11] and is position-controlled. CHIDORI has 6-axis force/torque sensors which we use for collision detection on each foot.

B. System Architecture

Fig.2 shows an overview of the control system. The system consists of the following three components:

1) Swing Foot Trajectory Regenerator (Blue block)
   This component regenerates a swing foot trajectory, a landing point and a reference ZMP on the basis of a swing foot collision state. Furthermore, it modifies subsequent foot trajectories.
2) Swing Foot Collision Detector (Red block)
   This component detects a foot collision by values of force sensors and a current time during swing phase.
3) Swing Foot Impact Mitigation Controller (Green block)
   This component mitigates the impact on a swing foot. It is composed of the following two controllers: Swing Foot Force Controller, which is the feedback controller using force sensors, and Feedback Gain of Swing Leg Joints Controller, which is the feedforward controller for the feedback gain of joints.

The details of component 1, 2 are explained in Section III. The detail of component 3 is explained in Section IV.

III. Swing Foot Trajectory Regeneration after Collision Detection

A. Smooth Foot Trajectory Generation

To begin with, we explain the basic method to generate foot trajectories. Before we generate the trajectories, we determine some control points as an outline of the trajectories. To generate acceleration continuous trajectories of swing foot from control points, we use Kanehiro *et al.*'s method[12] shown in Algorithm 1. $path$ is the shortest trajectory which passes control points from the foot position, t_{remain} is the time to land, $target$ is the point on the $path$ which arrives the goal t_{offset} earlier than the swing foot, Δt is the sampling time, and x, v, a stand for the foot position, velocity, acceleration respectively. Divide$(path, ratio)$ is the function which returns the point which divides $path$ in the ratio, and HoffArbib is the one which calculates x, v, a for

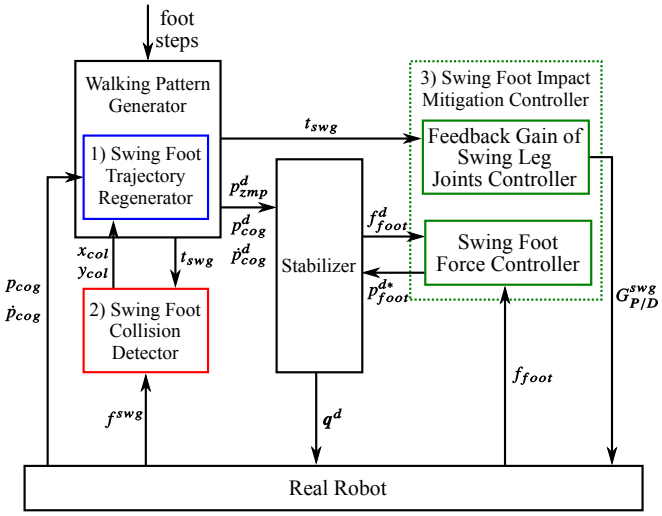

Fig. 2: System architecture of proposed controller against swing foot collision

Algorithm 1 calcSwingLegPosition$(path, t_{remain}, x, v, a)$

```
if t_remain > t_offset then
    target ← Divide(path, Δt/(t_remain − t_offset))
    HoffArbib(t_offset, target, x, v, a)
else
    target ← Divide(path, 1.0)
    HoffArbib(t_remain, target, x, v, a)
end if
```

the minimum jerk trajectory to $target$ by calculating jerk-level values from Eq.1[13].

$$\dot{a} = -9a/t - 36v/t^2 + 60(goal - x)/t^3 \qquad (1)$$

We are able to regenerate swing foot trajectories by changing control points. By resetting control points appropriately, we can generate the trajectories when the robot detects the swing foot collision.

B. Foot Trajectory Regeneration Depending on Situations

Here we classify the strategies for foot trajectory regeneration into two types as Fig.3. We explain each strategy as follows.

1) Return Foot from Collision Point: When humanoid robots collide with what they can not recognize due to poor environmental recognition, they should return the swing foot. However, to modify a landing point largely causes instability. Therefore we return the swing foot 50mm, which is shorter than stride length and enough length to avoid re-collision. At this time the regenerated swing foot trajectory is almost same as cycloid.

2) Continue Walking: Suppose the swing foot collided in spite of the footstep plan with environmental recognition such as stepping up stairs or striding over an obstacle. In this case, we are able to regenerate the swing foot trajectory to avoid the obstacle and continue walking by updating the

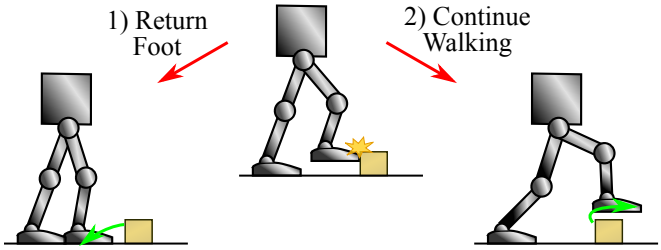

Fig. 3: Two strategies for foot trajectory regeneration after collision detection

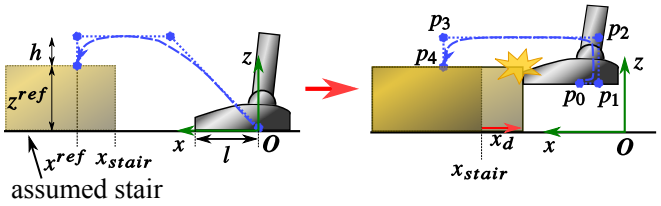

Fig. 4: Swing foot trajectory regeneration after foot collision to continue stepping up the stair

perception of environment. Fig.4 shows the case a stair is closer than expected, where x-axis is the moving direction. Let $\boldsymbol{p}_0$ be the swing foot position when the foot collided. Then the difference between an assumed and an actual position of stair is represented as Eq.2.

$$x_d = (\boldsymbol{p}_0 - \boldsymbol{O}) \cdot \boldsymbol{e}_x + l - x_{stair} \tag{2}$$

$$\text{where} \quad \boldsymbol{e}_x \coloneqq \begin{bmatrix} 1 & 0 & 0 \end{bmatrix} \tag{3}$$

Using x_d, we determine new control points $\boldsymbol{p}_1 - \boldsymbol{p}_4$ as follows.

$$\boldsymbol{p}_1 = \boldsymbol{p}_0 - x_{offset} \cdot \boldsymbol{e}_x \tag{4}$$

$$\boldsymbol{p}_2 = \begin{bmatrix} \boldsymbol{p}_1 \cdot \boldsymbol{e}_x & 0 & z + h \end{bmatrix}^T \tag{5}$$

$$\boldsymbol{p}_3 = \begin{bmatrix} x^{ref} + x_d & 0 & z^{ref} + h \end{bmatrix}^T \tag{6}$$

$$\boldsymbol{p}_4 = \begin{bmatrix} x^{ref} + x_d & 0 & z^{ref} \end{bmatrix}^T \tag{7}$$

Furthermore, we compensate the odometry error by shifting control points of subsequent footsteps by x_d. This method can apply to the case the humanoid robot strides over an obstacle.

C. Motion Generation after Foot Trajectory Regeneration

1) ZMP Tracking COG Trajectory Generation Using Preview Control: To generate a COG trajectory, we use preview control theory[14]. Using this theory, we are able to generate the COG trajectory which follows the new reference ZMP after foot trajectory regeneration.

Let $\begin{bmatrix} x_G & y_G & z_G \end{bmatrix}^T, \begin{bmatrix} x_Z & y_Z & z_Z \end{bmatrix}^T$ be the COG and ZMP, respectively. Assuming $\ddot{z}_G = 0$, x_Z is obtained by LIP dynamics.

$$x_Z = x_G - \frac{1}{\omega^2} \ddot{x}_G \tag{8}$$

$$\omega \coloneqq \sqrt{\frac{g}{z_G - z_Z}} \tag{9}$$

g is the gravitational acceleration. Regarding $\ddot{x}_G$ as the input, Eq.8 is represented as the following discrete dynamical system.

$$\begin{cases} \boldsymbol{x}_{k+1} &= \boldsymbol{A}\boldsymbol{x}_k + \boldsymbol{B}u_k \\ x_{Z,k} &= \boldsymbol{C}\boldsymbol{x}_k \end{cases} \tag{10}$$

$$\text{where} \quad \boldsymbol{x}_k = \begin{bmatrix} x_{G,k} & \dot{x_{G,k}} & \ddot{x_{G,k}} \end{bmatrix}^T, u_k = \dddot{x}_{G,k} \tag{11}$$

$$\boldsymbol{A} = \begin{bmatrix} 1 & \Delta t & \Delta t^2/2 \\ 0 & 1 & \Delta t \\ 0 & 0 & 1 \end{bmatrix}, \boldsymbol{B} = \begin{bmatrix} \Delta t^3/6 \\ \Delta t^2/2 \\ \Delta t \end{bmatrix} \tag{12}$$

$$\boldsymbol{C} = \begin{bmatrix} 1 & 0 & -1/\omega^2 \end{bmatrix} \tag{13}$$

To remove the ZMP offset error, Eq.10 is expanded as follows.

$$\begin{cases} \boldsymbol{x}^*_{k+1} &= \tilde{\boldsymbol{A}}\boldsymbol{x}^*_k + \tilde{\boldsymbol{B}}\Delta u_k \\ x_{Z,k} &= \tilde{\boldsymbol{C}}\boldsymbol{x}^*_k \end{cases} \tag{14}$$

$$\text{where} \quad \boldsymbol{x}^*_k = \begin{bmatrix} x_{Z,k} \\ \Delta \boldsymbol{x}_k \end{bmatrix} \tag{15}$$

$$\Delta \boldsymbol{x}^*_k = \boldsymbol{x}_k - \boldsymbol{x}_{k-1}, \Delta u_k = u_k - u_{k-1} \tag{16}$$

$$\tilde{\boldsymbol{A}} = \begin{bmatrix} 1 & \boldsymbol{C}\boldsymbol{A} \\ 0 & \boldsymbol{A} \end{bmatrix}, \tilde{\boldsymbol{B}} = \begin{bmatrix} \boldsymbol{C}\boldsymbol{B} \\ \boldsymbol{B} \end{bmatrix} \tag{17}$$

$$\tilde{\boldsymbol{C}} = \begin{bmatrix} 1 & 0 & 0 & 0 \end{bmatrix} \tag{18}$$

With the given reference ZMP $x^{ref}_{Z,k+i}$ at the time $i\Delta t$, the performance index is specified as

$$J = \sum_{i=k}^{\infty} \left\{ Q(x^{ref}_{Z,i} - x_{Z,i})^2 + R\Delta u_i^2 \right\} \tag{19}$$

When the reference ZMP can be previewed for N steps, the input which minimizes Eq.19 is calculated as below.

$$\Delta u_k = -\tilde{\boldsymbol{K}}\boldsymbol{x}^*_k + \sum_{i=1}^{N} \tilde{f}_i x^{ref}_{Z,k+i} \tag{20}$$

Where $\tilde{\boldsymbol{K}}, \tilde{f}_i$ are the gains calculated from the weights Q, R and the system parameter. The system input u_k is obtained from Eq.20.

$$u_k = -\tilde{\boldsymbol{K}} \sum_{j=0}^{k} \boldsymbol{x}^*_j + \sum_{j=0}^{k} \sum_{i=1}^{N} \tilde{f}_i x^{ref}_{Z,j+i} \tag{21}$$

The input for y-direction is obtained in the same way.

2) Landing Point Modification Based on Capture Point: Although we generate the COG trajectory by preview control theory, a change of landing point may cause ZMP tracking failure. For the robot to avoid falling down, we use the online landing point modification method[15] based on Capture Point[4][5]. The correction value of the landing point after L steps to reduce Capture Point (x_ξ) errors is calculated as below.

$$\delta x^{ref}_Z = (\sum_{i=L}^{N} \tilde{f}_i)^{-1} (\boldsymbol{D}\boldsymbol{B})^{-1} k_\xi \left(x^{act}_\xi - x^{ref}_\xi \right) \tag{22}$$

$$\text{where} \quad \boldsymbol{D} = \begin{bmatrix} 1 & 1/\omega & 0 \end{bmatrix} \tag{23}$$

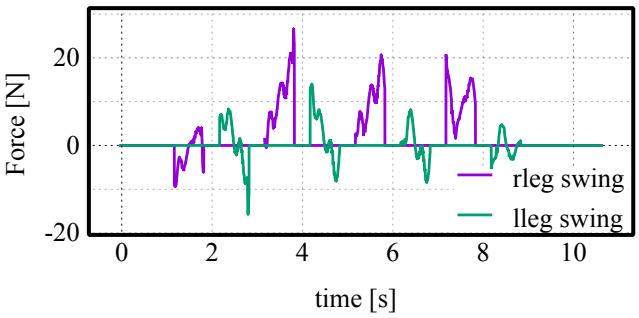

Fig. 5: Forward swing foot force during walking by CHIDORI. Each step lasts 1.0 seconds, and a stride is 0.15 meters. Large force is applied at the beginning and end of the swing phase.

k_ξ is a constant gain. If $|x_\xi^{act} - x_\xi^{ref}|$ is exceeds a threshold ξ^{thre}, we modify the landing point by Eq.22. However, when the robot is returning the swing foot (III-B.1), we should take care of re-collision. For this reason we limit the modified landing point to the regenerated point in the moving direction.

D. Swing Foot Collision Detection

Fig.5 shows forward swing foot force during walking by CHIDORI. It shows swing foot force is less than about 20N, therefore we determine the threshold of collision detection to 60N in order not to get a false positive detection by difference of walking conditions and measurement errors.

As shown in Fig.5, large force is applied at the beginning and end of the planned swing phase. This force is due to the discrepancy between the planned and actual grounding state of the foot. This may cause a false positive detection, therefore we set the dead zone of 0.1s at both ends.

Eq.24 shows the collision detection in x-axis direction.

$$x_{collision} = True \quad \text{if} \quad |f_x^{swg}| \geq F_x^{thre} \text{ and } t_{swg} \in T_{detect} \tag{24}$$

t_{swg} is the current time of swing phase. The collision in y-direction is able to be detected in the same way.

IV. Swing Foot Impact Mitigation Controller

A. Swing Foot Force Controller

The swing foot force controller modifies foot positions to realize the desired foot forces. We expand the foot force difference control[1] to the swing foot.

To begin with, we define a function which returns a control value δ_k.

$$\begin{aligned} &\text{damping}(f^d, f, D, T) \coloneqq \delta_{k-1} + \dot{\delta}_{k-1}\Delta t \\ &= \delta_{k-1} + \left(D^{-1}(f^d - f) - \frac{1}{T}\delta_{k-1} \right) \Delta t \end{aligned} \tag{25}$$

where f, D, T are input value, damping gain and time constant respectively. In addition, the superscript d indicates a desired value.

Let p_x, f_x, D_x be the x component of the foot position, foot force, and damping gain. The superscript $d*$ and the subscript L, R indicate the modified desired value, left and right foot value respectively. Although the following equations are formulated for the x component, they apply to the y and z component as well. Using Eq.25, we modify the foot positions as follows.

$$\Delta p_x = \text{damping}\left(f_{xL}^d - f_{xR}^d, f_{xL} - f_{xR}, D_x, T\right) \tag{26}$$

$$p_{xR}^{d*} = p_{xR}^d + 0.5\Delta p_x \tag{27}$$

$$p_{xL}^{d*} = p_{xL}^d - 0.5\Delta p_x \tag{28}$$

To mitigate collision impact without causing oscillation, we change D_x depending on difference between desired and actual foot force.

$$D_x = \begin{cases} D_x^{sup} & \left(\left| f_{diff}^d - f_{diff}^{act} \right| < F_x \right) \\ D_x^{swg} & \left(\left| f_{diff}^d - f_{diff}^{act} \right| \geq F_x \right) \end{cases} \tag{29}$$

$$\text{where } D_{swg} < D_{sup}, \;\; f_{diff} \coloneqq f_{xL} - f_{xR}$$

In horizontal direction, F_x, F_y are the same as the threshold of collision detection F_x^{thre}, F_y^{thre}.

B. Feedback Gain of Swing Leg Joints Controller

Just using the swing foot force controller, however, the damping gain causes response delay. Therefore, to reduce a strong impact, we propose the method to control the feedback P/D gain of swing leg joints. As the previous study, Tajima *et al.* [16] proposed this method to absorb landing impact. However, landing on the leg whose feedback gain is reduced causes instability of walking. Therefore we finish increasing the gains before landing. In addition, the increase of the gains linearly to avoid a sudden change of joint angles.

$$G_{P/D}^{swg} = \begin{cases} G_{P/D}^{low} \quad (0 \leq t_{swg} \leq t_s) \\ \text{Linear}(G_{P/D}^{swg}, G_{P/D}^{org}, t_{swg}, t_s, t_e) \\ \qquad\qquad (t_s < t_{swg} \leq t_e) \end{cases} \tag{30}$$

$G_{P/D}^{swg}, G_{P/D}^{low}, G_{P/D}^{org}, t_s, t_e$ are the current gains of swing leg joints, the lowest gains, the original gains before reducing, the beginning and the end time of increasing phase, respectively. $\text{Linear}()$ is the function for linear interpolation.

V. Experiments of the Biped Robot against Two Types of Collision Situations

A. Return the Foot on the Flat Ground

We carried out some stumble experiments with CHIDORI. As shown in Fig.6, CHIDORI fell down with yaw rotation without regenerating a swing foot trajectory. With the regeneration, however, CHIDORI successfully avoided falling down (Fig.7). As can be seen from Fig.8 and Fig.9, the method was able to reduce yaw rotation and maximum swing foot force.

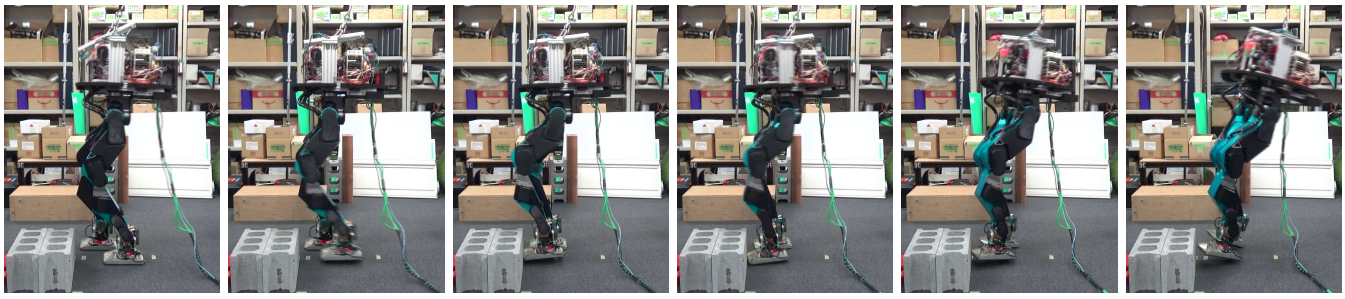

(a) $t = 0.0$s (b) $t = 0.3$s (c) $t = 0.6$s (d) $t = 0.7$s (e) $t = 1.0$s (f) $t = 1.3$s

Fig. 6: Swing foot collision during walking on a horizontal plane without swing foot regeneration and CHIDORI fell down. Each step lasts 1.2 seconds, and a stride is 0.15 meters.

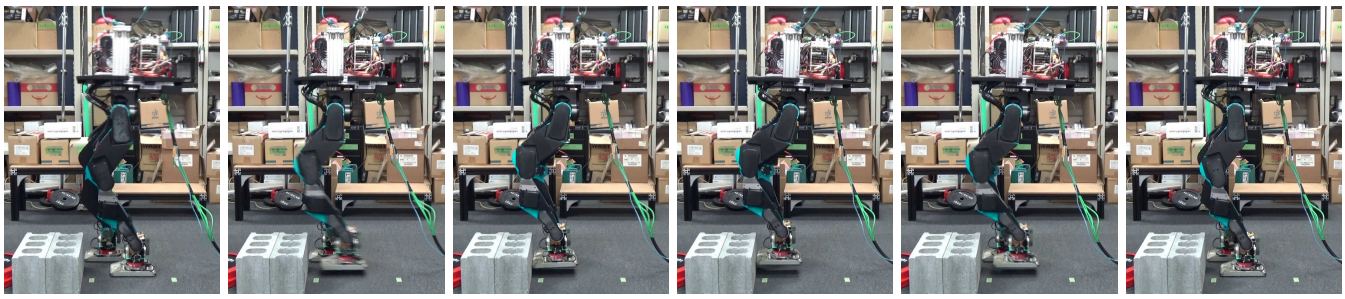

(a) $t = 0.0$s (b) $t = 0.3$s (c) $t = 0.6$s (d) $t = 1.0$s (e) $t = 1.3$s (f) $t = 1.7$s

Fig. 7: Swing foot collision during walking on a horizontal plane with swing foot collision detection and regenerate swing foot trajectory. Each step lasts 1.2 seconds, and a stride is 0.15 meters.

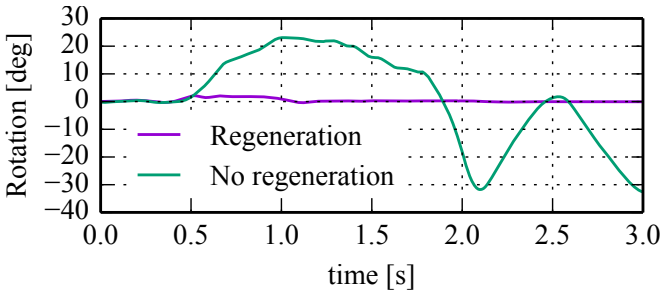

Fig. 8: Base-link yaw posture during walking on the flat ground when foot collided. The swing foot regeneration reduced yaw rotation.

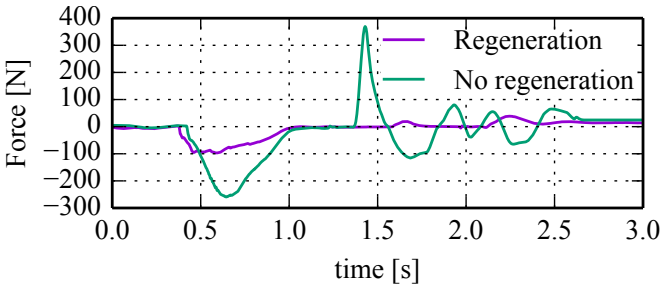

Fig. 9: X component of the swing foot force during walking on the flat ground when foot collided. The swing foot regeneration reduced swing foot force.

B. *Continue Stepping Up the Stair*

We also conducted the experiments of stepping up the stair which is 290mm tall and 120mm from the toes. As shown in Fig.10, CHIDORI fell down with yaw and pitch rotation without regenerating a swing foot trajectory. With the regeneration and impact mitigation, however, CHIDORI successfully avoided falling down and continued stepping up (Fig.11). In addition to the swing foot trajectory regeneration, we validate the impact mitigation control in the following four cases:

1) With all of impact mitigation control (= 2) + 3))
2) With feedback gain of swing leg joint control
3) With swing foot force control
4) No mitigation control

TABLE I: Feedback P/D gain of each joint

Joint	G_P^{org} [Nm/rad]	G_P^{swg} [Nm/rad]	G_D^{org} [Nms/rad]	G_D^{swg} [Nms/rad]
Hip Yaw	$3.24 \cdot 10^4$	$1.62 \cdot 10^3$	$1.47 \cdot 10^2$	7.35
Hip Roll	$8.31 \cdot 10^4$	$4.16 \cdot 10^3$	$3.76 \cdot 10^2$	$1.88 \cdot 10$
Hip Pitch	$6.49 \cdot 10^4$	$3.25 \cdot 10^3$	$1.47 \cdot 10^2$	7.35
Knee Pitch	$6.49 \cdot 10^4$	$3.25 \cdot 10^3$	$1.47 \cdot 10^2$	7.35
Ankle Pitch	$4.67 \cdot 10^4$	$2.34 \cdot 10^3$	$2.11 \cdot 10^2$	$1.06 \cdot 10$
Ankle Roll	$3.29 \cdot 10^4$	$1.65 \cdot 10^3$	$1.49 \cdot 10^2$	7.45

Here we set the damping gains in Eq.29 as $D_x^{sup} = 16800\text{Ns/m}, D_x^{swg} = 840\text{Ns/m}$, and the gain of joints in Eq.30 as Table I.

Fig.12 and Fig.13 show the swing foot force and yaw rotation in each case. We can see the feedback gain of swing leg joint control reduced the maximum impact force and posture

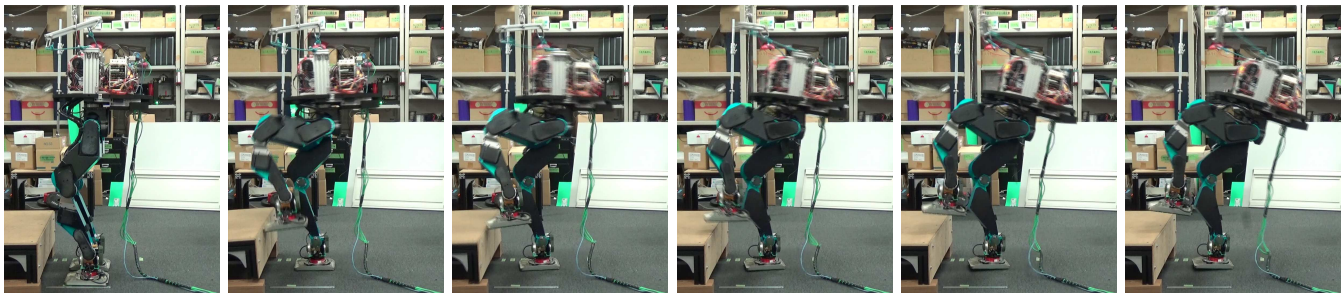

(a) $t = 0.0$s (b) $t = 0.5$s (c) $t = 0.6$s (d) $t = 0.7$s (e) $t = 0.8$s (f) $t = 0.9$s

Fig. 10: Swing foot collides during stepping up the stair with no detection and fell down with yaw and pitch rotation. Each step lasts 1.4 seconds.

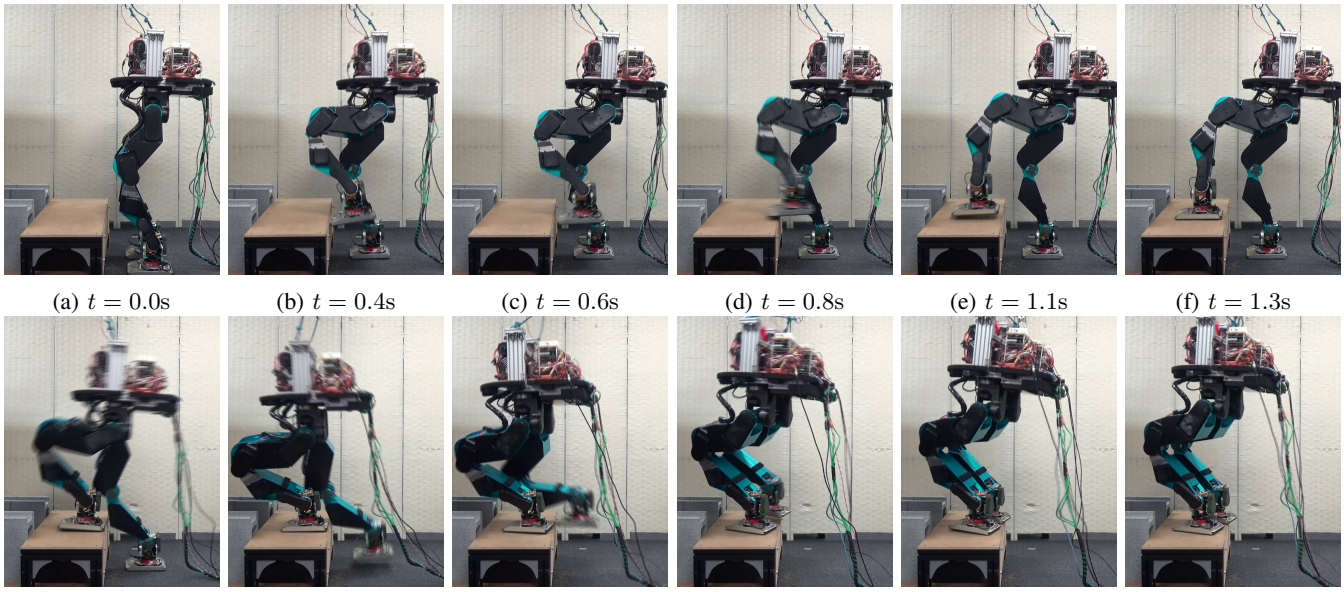

(a) $t = 0.0$s (b) $t = 0.4$s (c) $t = 0.6$s (d) $t = 0.8$s (e) $t = 1.1$s (f) $t = 1.3$s

(g) $t = 1.9$s (h) $t = 2.1$s (i) $t = 2.3$s (j) $t = 2.5$s (k) $t = 2.7$s (l) $t = 3.0$s

Fig. 11: Swing foot collides during stepping up the stair with impact mitigation. CHIDORI succeeded to continue stepping up with the foot trajectory regeneration. Each step lasts 1.3 seconds.

rotation. On the other hand, due to the response delay, the swing foot force control doesn't reduce the maximum impact force compared to the no mitigation control. However, with the force control, the swing foot force decreases faster. This result causes the decrease of yaw rotation in Fig.13. Fig.14 shows the swing foot trajectory in the case of (1). We can see the left foot trajectory was regenerated after collision, and the right foot trajectory was also regenerated in order to avoid collision.

VI. CONCLUSION

In this paper, we proposed bipedal walking controller against swing foot collision. This controller is composed of following three components: Swing Foot Trajectory Regenerator, Swing Foot Collision Detector and Swing Foot Impact Mitigation Controller. For foot trajectory regeneration, we explained how to reset control points on the basis of two types of strategies. To detect collision of the swing foot, we determined the threshold and the dead zone of collision detection during walking by the real robot. To mitigate strong impact, we proposed the foot-force feedback controller and the joint-gain feedforward controller. These methods were validated through the experiments. Against the collision during walking on the flat ground, our experimental humanoid robot CHIDORI successfully returned the swing foot and came to stop. Against the collision during stepping up the stair, CHIDORI successfully continued stepping up by regenerating foot trajectories. In addition, through this experiment, we confirmed the effect of the impact mitigation controller. The joint-gain control reduced the maximum impact force and posture rotation. On the other hand, the foot-force control did not reduce the maximum impact force, however, reduced the impact force faster. Finally, the impact mitigation controller reduced the maximum impact force by 20N, and the maximum base-link yaw rotation by 4°.

However, the foot trajectory regeneration is limited to 2D plane. In addition, the swing foot collision detection

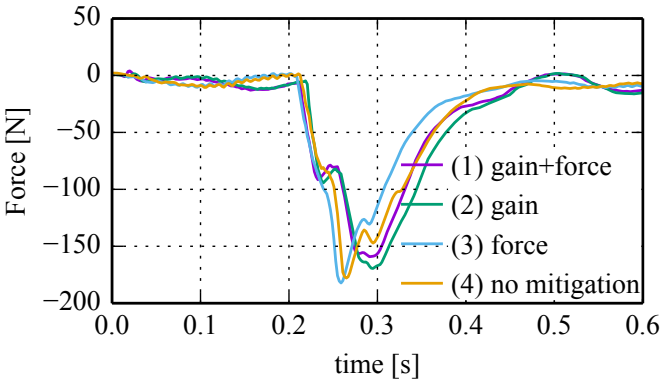

Fig. 12: X component of the swing foot force before and after the collision during the stepping-up experiment (1) to (4). The joint-gain control reduces the maximum impact force and the foot-force control reduces the foot force faster.

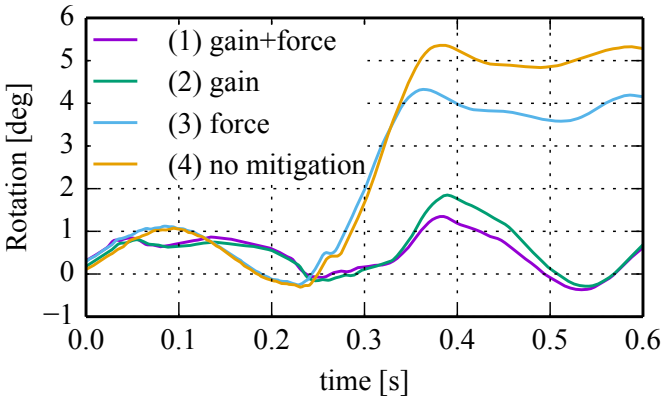

Fig. 13: Base-link yaw posture before and after the collision during the stepping-up experiment (1) to (4). Foot-force control reduces the maximum yaw rotation.

is implemented empirically and needs to be validated in more complex situations. In the future work, we desire to expand the foot trajectory regeneration into 3D-trajectory for more complicated environment, combining with environmental recognition.

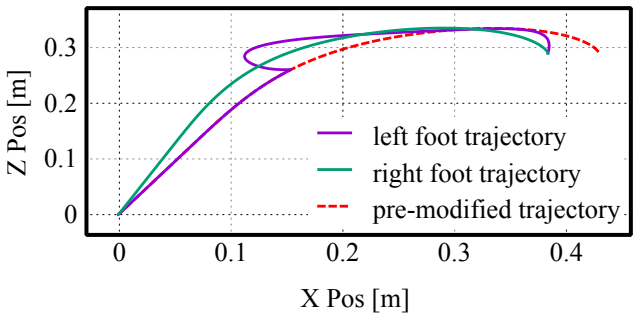

Fig. 14: Vertical position of swing foot trajectory with respect to x position. The pre-modified trajectory corresponds to both left and right foot trajectories. The left foot trajectory is regenerated after collision, and the right foot trajectory is also regenerated in order to avoid collision.

References

[1] S. Kajita, M. Morisawa, K. Miura, S. Nakaoka, K. Harada, K. Kaneko, F. Kanehiro, and K. Yokoi. Biped walking stabilization based on linear inverted pendulum tracking. In *Proceedings of the 2010 IEEE/RSJ International Conference on Intelligent Robots and Systems*, pp. 4489–4496, 2010.

[2] Shuuji Kajita, Fumio Kanehiro, Kenji Kaneko, Kazuhito Yokoi, and Hirohisa Hirukawa. The 3d linear inverted pendulum mode: A simple modeling for a biped walking pattern generation. In *Proceedings of the IEEE/RSJ International Conference on Intelligent Robots and Systems*, Vol. 1, pp. 239–246, 2001.

[3] Koichi Nishiwaki and Satoshi Kagami. Walking control on uneven terrain with short cycle pattern generation. In *Proceedings of the IEEE-RAS International Conference on Humanoid Robots*, pp. 447–453, 2007.

[4] Jerry Pratt, John Carff, Sergey Drakunov, and Ambarish Goswami. Capture Point: A Step toward Humanoid Push Recovery. In *Proceedings of the IEEE-RAS International Conference on Humanoid Robots*, pp. 200–207, Dec 2006.

[5] Benjamin Stephens. Humanoid push recovery. In *Proceedings of the IEEE-RAS International Conference on Humanoid Robots*, pp. 589–595, 2007.

[6] Tomomichi Sugihara. Standing stabilizability and stepping maneuver in planar bipedalism based on the best com-zmp regulator. In *Proceedings of the IEEE International Conference on Robotics and Automation*, pp. 1966–1971, 2009.

[7] Mitsuharu Morisawa, Fumio Kanehiro, Kenji Kaneko, Shuuji Kajita, and Kazuhiro Yokoi. Reactive biped walking control for a collision of a swinging foot on uneven terrain. In *Proceedings of the IEEE-RAS International Conference on Humanoid Robots*, pp. 768–773, 2011.

[8] Gill A Pratt and Matthew M Williamson. Series elastic actuators. In *Proceedings of the IEEE/RSJ International Conference on Intelligent Robots and Systems*, Vol. 1, pp. 399–406, 1995.

[9] Johannes Englsberger, Alexander Werner, Christian Ott, Bernd Henze, Maximo A Roa, Gianluca Garofalo, Robert Burger, Alexander Beyer, Oliver Eiberger, Korbinian Schmid, et al. Overview of the torque-controlled humanoid robot toro. In *Proceedings of the IEEE-RAS International Conference on Humanoid Robots*, pp. 916–923, 2014.

[10] Yoshito Ito, Shunich Nozawa, Junichi Urata, Takuya Nakaoka, Kazuya Kobayashi, Yuto Nakanishi, Kei Okada, and Masayuki Inaba. Development and verification of life-size humanoid with high-output actuation system. In *Proceedings of the IEEE International Conference on Robotics and Automation*, pp. 3433–3438, May 2014.

[11] Junichi Urata, Toshinori Hirose, Namiki Yuta, Yuto Nakanishi, Ikuo Mizuuchi, and Masayuki Inaba. Thermal control of electrical motors for high-power humanoid robots. In *Proceedings of the 2008 IEEE/RSJ International Conference on Intelligent Robots and Systems*, pp. 2047–2052, 2008.

[12] Fumio Kanehiro, Mitsuharu Morisawa, Wael Suleiman, Kenji Kaneko, and Eiichi Yoshida. Reactive Leg Motion Generation Method under Consideration of Physical Constraints. *Journal of the Robotics Society of Japan*, Vol. 28, No. 10, pp. 1251–1261, 2010. (Japanese).

[13] B. Hoff and M. A. Arbib. Models of trajectory formation and temporal interaction of reach and grasp. *Journal of Motor Behavior*, Vol. 25, No. 3, pp. 175–192, 1993.

[14] S. Kajita, F. Kanehiro, K. Kaneko, K. Fujiwara, K. Harada, K. Yokoi, and H. Hirukawa. Biped walking pattern generation by using preview control of zero-moment point. In *Proceedings of the 2003 IEEE International Conference on Robotics and Automation*, Vol. 2, pp. 1620–1626, 2003.

[15] Yuta Kojio, Tatsushi Karasawa, Kunio Kojima, Ryo Koyama, Fumihito Sugai, Shunichi Nozawa, Yohei Kakiuchi, Kei Okada, and Masayuki Inaba. Walking control in water considering reaction forces from water for humanoid robots with a waterproof suit. In *Proceedings of the IEEE/RSJ International Conference on Intelligent Robots and Systems*, pp. 658–665, 2016.

[16] Ryosuke Tajima, Daisaku Honda, and Keisuke Suga. Fast running experiments involving a humanoid robot. In *Proceedings of the IEEE International Conference on Robotics and Automation*, pp. 1571–1576, 2009.